Velocity control of mini-UAV using a helmet system

Jose Juan Téllez-Guzmán, Jose-Ernesto Gomez-Balderas, Nicolas Marchand, Pedro Castillo, J Colmenares Vazquez, Jonatan Álvarez-Muñoz, Jonathan Dumon

Velocity control of mini-UAV using a helmet system

J.J. Tellez-Guzman[1], J.E. Gomez-Balderas[1], N. Marchand[1,2], P. Castillo[3], J. Colmenares Vazquez[1], J.U. Alvarez-Munoz[1] and J. Dumon[1]

***Abstract*— The usage of a helmet to command a mini-unmanned aerial vehicle (mini-UAV), is a telepresence system that connects the operator to the vehicle. This paper proposes a system which remotely allows the connection of a pilot's head motion and the 3D movements of a mini-UAVs. Two velocity control algorithms have been tested in order to manipulate the system. Results demonstrate that these movements can be used as reference inputs of the controller of the mini-UAV.**

I. INTRODUCTION

Sensory perception is one of the most important problems with the remote operation of flying vehicles. It is considerably increased when the operator is not physically or virtually connected with the vehicle in flight. In many cases designers attempt to ameliorate the sensorless deficit by equipping the vehicle with an onboard camera to augment the sensitivity of the environment in which it operates. This makes the mini-UAV susceptible to collision in lateral, vertical, and rear directions.

A novel semiautonomous haptic teleoperation control architecture for multiple UAVs is proposed in [1], [2]. In [3] authors introduces a novel framework for semi-autonomous path corrections using a haptic feedback algorithm in which the force is not explicitly given by the motion of the robot. Rather mouvements depends on the teleoperated path. Haptic feedback can be used to complement visual feedback [4]. The free and open source Tele-Operation Platform of the MPI for Biological Cybernetics (TeleKyb) is used for the development of bilateral teleoperation systems between human interfaces and groups of mini-UAVs [5]. Nevertheless, only few works until now have been made completely autonomous. For example, a semi-autonomous UAV for indoor teleoperation using RGB-D as exteroceptive sensor is used for pose estimation in [6]. Vision-Based Position Control and Optic flow-based Vision system for 3D localization and control of small aerial vehicles has been developed in [7]. A study to integrate humans and machines with different habilities (i.e, flying) to virtually augment human habilities has been made in [8]. In [9] an Ar.Drone is controlled through head position and gestures performed by operator wearing a google glass.

In this work we develop and implement a mini-UAV system controlled by a portable helmet. the diagram of the system is depicted in Fig.1. The mini-UAV has an IMU to obtain the attitude quaternion and angular velocity. However, to obtain the states of position and linear velocity, we need any extra devices (GPS, cameras, flow optics sensors). A communication system is necessary to swap out information between the mini-UAV and the ground station. A PC computes the velocity control algortihm of mini-UAV. The data of the portable helmet will be processed by the PC ground station that will serve as a reference for the control law.

The paper is organized as follows. First in section II we describe the heading control. In section III we present some mathematical definitions and the velocity control strategy for nonlinear systems. Some experimental results are presented in section IV and discussions finally conclude the paper.

II. HEADING CONTROL

One of the characteristics of the head control with regard to UAV control is that the operators can intuitively determine the position and the orientation of the mini-UAV. The operator wears a helmet and he can tilt his head to obtain the references of control. With these head motions, the operator can intuitively manipulate an UAV. When the operator tilts his head in front or back (see Fig. 2(a) and 2(b)), right or left (see Fig. 2(c) and 2(d)) the UAV flies in the same direction. When the operator rotates his head, the UAV rotates in the same direction.

III. SYSTEM MODEL AND VELOCITY CONTROL

A. System model

The mini-UAV is a small aerial vehicle. It is lifted and propelled, forward and laterally, by controlling the rotational speed of four blades mounted at the four ends of a simple cross and driven by four DC Brushed motors. On such a platform (see Fig. 3), given that the front and rear motors rotate counter-clockwise while the other two rotate clockwise, gyroscopic effects and aerodynamic

∗ This work was supported by LabEx PERSYVAL-Lab (ANR-11-LABX-0025), Equipex ROBOTEX (ANR-10-EQPX-44-01) and by GIPSA-Lab in France

[1] Univ. Grenoble Alpes, GIPSA-Lab, FR-38000 Grenoble, France. (e-mail: jose-juan.tellez-guzman@gipsa-lab.grenoble-inp.fr, Nicolas.Marchand@gipsa-lab.grenoble-inp.fr, jose-ernesto.gomez-balderas@gipsa-lab.grenoble-inp.fr)

[2] CNRS, GIPSA-Lab, FR-38000 Grenoble, France. (e-mail:Nicolas.Marchand@gipsa-lab.grenoble-inp.fr)

[3] UMI LAFMIA, CNRS (e-mail:pedro.castillo@hds.utc.fr)

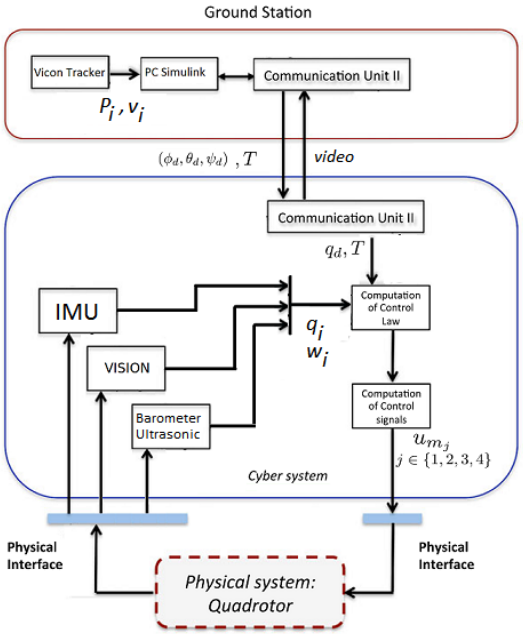

Fig. 1: Diagram System

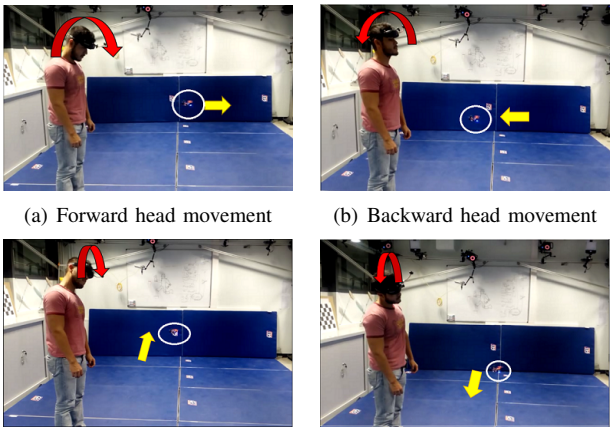

(a) Forward head movement (b) Backward head movement

(c) Left head movement (d) Right head movement

Fig. 2: Teleoperation with head movements

torques tend to cancel each other in trimmed flight. The rotation of the four rotors generates a vertical force, called the thrust T, equal to the sum of the thrusts of each rotor ($T = f_1 + f_2 + f_3 + f_4$). The pitch movement θ is obtained by increasing/decreasing the speed of the rear motor while decreasing/increasing the speed of the front motor. The roll movement ϕ is obtained similarly using the lateral motors. The yaw movement ψ is obtained by increasing/decreasing the speed of the front and rear motors while decreasing/increasing the speed of the lateral motors. In order to avoid any linear movement of the mini-UAV, these maneuvers should be achieved while maintaining a value of the total thrust T which balances the aircraft weight. In order to modelize the dynamics system, two frames are defined: a fixed frame in the space $\mathbf{E}^f = [\vec{e}_1{}^f, \vec{e}_2{}^f, \vec{e}_3{}^f]$ and a body-fixed frame $\mathbf{E}^b = [\vec{e}_1{}^b, \vec{e}_2{}^b, \vec{e}_3{}^b]$, attached to the mini-UAV at its center of gravity, as shown in Fig. 3.

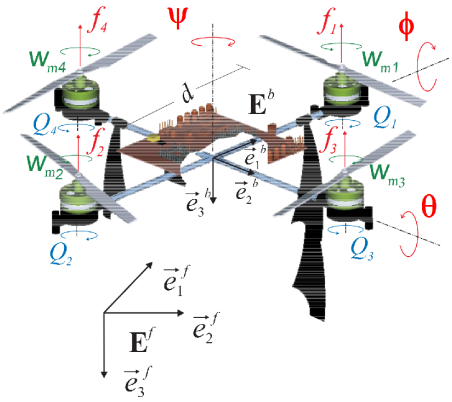

Fig. 3: Quadrotor: fixed frame $\mathbf{E}^f = [\vec{e}_1^f, \vec{e}_2^f, \vec{e}_3^f]$ and body-fixed frame $\mathbf{E}^b = [\vec{e}_1^b, \vec{e}_2^b, \vec{e}_3^b]$

According to [10], the six degrees of freedom model (position and attitude) of the system can be separated into translational and rotational motions, represented respectively by Σ_T and Σ_R in equations (1) and (2).

$$\Sigma_T : \begin{cases} \dot{\vec{p}} = \vec{v} \\ m\dot{\vec{v}} = -m\vec{g} + RF \end{cases} \tag{1}$$

$$\Sigma_R : \begin{cases} \dot{q} = \frac{1}{2}\Xi(q)\omega \\ J\dot{\omega} = -[\omega^\times]J\omega + \Gamma \end{cases} \tag{2}$$

where m denotes the mass of the mini-UAV, J its inertial matrix expressed in $\mathbf{E}^b$. R is the rotation matrix eq.(17). F is the total thrust eq.(16). g is the gravity acceleration and $e_3 = (0\ 0\ 1)^T$, $\vec{p} = (x\ y\ z)^T$ represents the position of the mini-UAV's center of gravity, which coincides with the origin of frame $\mathbf{E}^b$, with respect to frame $\mathbf{E}^f$, $v = (v_x\ v_y\ v_z)^T$ its linear velocity in $\mathbf{E}^f$, q is the orientation quaternion and ω denotes the angular velocity of the mini-UAV expressed in $\mathbf{E}^b$. $\Gamma \in \mathbb{R}^3$ depends on the couples generated by the actuators, aerodynamic couples and external couples (environmental forces).

The reactive torque Q_j due to the j^{th} rotor drag, $j \in \{1, 2, 3, 4\}$, and the total thrust T generated by the four rotors can be approximated by an algebraic relationship on function of a PWM control signal of the board :

$$Q_j = k_m \omega_{mj} \quad , \quad T = b_m \sum_{j=1}^{4} \omega_{mj} = \sum_{j=1}^{4} f_j \tag{3}$$

where the input signals ω_{mi} are angular rates. $k_m > 0$ and $b_m > 0$ are two parameters that depend on the air density,

the dynamic pressure, the lift coefficient, the radius and the angle of attack of the blades and they are obtained experimentally.

The components of the control torque vector Γ generated by the rotors are given by:

$$\begin{aligned}\Gamma_1 &= db_m(\omega_{m4} - \omega_{m3}) \\ \Gamma_2 &= db_m(\omega_{m1} - \omega_{m2}) \\ \Gamma_3 &= k_m(-\omega_{m1} - \omega_{m2} + \omega_{m3} + \omega_{m4})\end{aligned} \tag{4}$$

with d being the distance from one rotor to the center of mass of the mini-UAV. Combining equations (3) and (4), the forces and torques applied to the mini-UAV are written as:

$$\begin{pmatrix} \Gamma \\ T \end{pmatrix} = \begin{pmatrix} 0 & 0 & -db_m & db_m \\ db_m & -db_m & 0 & 0 \\ -k_m & -k_m & k_m & k_m \\ b_m & b_m & b_m & b_m \end{pmatrix} \begin{pmatrix} \omega_{m1} \\ \omega_{m2} \\ \omega_{m3} \\ \omega_{m4} \end{pmatrix} = NU_m$$

where $U_m = (\omega_{m1} \quad \omega_{m2} \quad \omega_{m3} \quad \omega_{m4})^T$. Since N is an invertible matrix, the vector of signals control U_m is easily obtained.

B. Attiude Control Design

1) Problem statement: The objective is to design a control law which drives the rigid body attitude to a specified constant orientation and maintains this orientation starting from any initial condition. It follows that the angular velocity vector must be brought to zero and remains null. Let q_d denotes the desired constant rigid body orientation, the control objective is then described by the following asymptotic condition:

$$q \to q_d,\ w \to 0 \text{ as } t \to \infty \tag{5}$$

2) Bounded attitude control: In this subsection, a control law which stabilizes the system described by (2) is proposed. The goal is to design a bounded control torque.

Definition 3.1: Given a positive constant M, a continuous, nondecreasing function saturation $\sigma_M : \mathbb{R} \to \mathbb{R}$ is defined by

$$\sigma_M := \begin{cases} s \text{ if } |s| < M \\ \text{sign}(s)M \text{ elsewhere} \end{cases} \tag{6}$$

Note that the components of Γ_{arm_i} are always bounded, *i.e.* $\mid \Gamma_{arm_i} \mid < \delta_i$. Then, we have the following result.

Consider the mini-UAV rotational dynamics described by Eqs. (2) with the following bounded control inputs:

$$\Gamma_i = -\sigma_{\overline{\Gamma}_i}\left(\frac{k\omega_i}{\rho_i} + sign(q_{e_0})kq_{e_i}\right) \tag{7}$$

where $\sigma(\cdot)$ are saturation functions as defined above. $\overline{\Gamma}_i$ with $i \in 1, 2, 3$ represents the physical bound on the $i\text{-}th$ torque Γ_i. k is a real parameter such that $0 < k \leq min_i\overline{\Gamma}_i/2$. ρ_i are strictly positive real parameters. Then the inputs in (7) almost globally asymptotically stabilize the rigid body to the origin ($q_{e_0} = 1, \vec{q_e} = 0$ and $\vec{\omega_e} = 0$).

The proof of this control law was made in [10].

C. Velocity Control

The test of the teleoperation was done with two algorithms which were taken from previous works. The first one is using a Boundary velocity control and the second one is using a Control Law for Trajectory Tracking.

1) Boundary velocity control: Dynamics of the whole system is obtained with the Newton-Euler formalism and the kinematics is represented using the quaternions formalism, and is given by (2) and (1). Note that the rotation matrix R can be given in function of Euler angles, as shown in [11].

Taking into account the equations (1) and (2), this system can be seen as a cascade system, where the translational dynamics (1), depends on the attitude (2), but the attitude dynamics does not depend on the translational one. This property will be used to design the control law. Now, assume that using the control law (7) one can stabilize the yaw dynamics, that is $\psi = 0$, then after a sufficiently long time, system (1) becomes:

$$\begin{pmatrix} \dot{p}_x \\ \dot{p}_y \\ \dot{p}_z \end{pmatrix} = \begin{pmatrix} v_x \\ v_y \\ v_z \end{pmatrix}, \tag{8}$$

$$\begin{pmatrix} \dot{v}_x \\ \dot{v}_y \\ \dot{v}_z \end{pmatrix} = \begin{pmatrix} -\frac{u}{m_T}\text{sen}\theta \\ \frac{u}{m_T}\text{sen}\phi\ \cos\theta \\ \frac{u}{m_T}\cos\phi\ \cos\theta - g \end{pmatrix}, \tag{9}$$

With an appropriate choice of these target configuration, it will be possible to transform (8) and (9) into three independent linear triple integrators. For this, take

$$\begin{aligned}\phi_d &:= \arctan\left(\frac{r_2}{r_3 + g}\right), \\ \theta_d &:= \arcsin\left(\frac{-r_1}{\sqrt{r_1^2 + r_2^2 + (r_3 + g)^2}}\right)\end{aligned} \tag{10}$$

where r_1, r_2 and r_3 will be defined later. Then, choose as positive thrust the input control

$$u = m\sqrt{r_1^2 + r_2^2 + (r_3 + g)^2} \tag{11}$$

Let be the state $p = (p_1, p_2, p_3, p_4, p_5, p_6) = (p_x, v_x, p_y, v_y, p_z, v_z)$, then (8) and (9) becomes:

$$\Sigma_x : \begin{cases} \dot{p}_1 = p_2 \\ \dot{p}_2 = r_1 \end{cases} \tag{12}$$

$$\Sigma_y : \begin{cases} \dot{p}_3 = p_4 \\ \dot{p}_4 = r_2 \end{cases} \tag{13}$$

$$\Sigma_z : \begin{cases} \dot{p}_5 = p_6 \\ \dot{p}_6 = r_3 \end{cases} \tag{14}$$

Note that u will be always positive, and $u \geq mg$, in order to compensate the system's weight.

Since the chains of integrators given in (12)-(14) have the same form, a control law can be proposed as in [12], and can be established by the next lemma:

Lemma 3.2: Taking into account the dynamics expressed in (12)-(14), the control laws with bounded inputs are given by

$$\begin{aligned} r_1 &:= -\vartheta\{a_2\sigma_M[\frac{1}{\vartheta}(a_1 p_1 + p_2) + a_1\sigma_M(\frac{1}{\vartheta}(p_2))]\} \\ r_2 &:= -\vartheta\{a_2\sigma_M[\frac{1}{\vartheta}(a_1 p_3 + p_4) + a_1\sigma_M(\frac{1}{\vartheta}(p_4))]\} \\ r_3 &:= -\vartheta\{a_2\sigma_M[\frac{1}{\vartheta}(a_1 p_5 + p_6) + a_1\sigma_M(\frac{1}{\vartheta}(p_6))]\} \end{aligned} \tag{15}$$

where $\sigma_M(\cdot)$ is defined in (6), with $M = 1$, $(a_1, a_2) > 0$ are tuning parameters defined before, and ϑ is given by $\vartheta = \bar{r}/(a_1 + a_2)$ being $\bar{r}$ the maximun value that can take the signals r_i.

Then, the control laws in (15) exponentially stabilize the systems (12)-(14) to the desired position and desired velocity, i.e. $t \to \infty, p = 0$.

2) Control Law for Trajectory Tracking: The approach used for the trajectory tracking is based in the backstepping technique. To ensure the convergence to desired trajectory using the backstepping design a integral control. The integral control helps to reduce the error of the tracking and add a factor to improve the robustness when parameters of the system are not well-known. In the next lines will describe the control strategy.

The thrust vector F and weight vector F_g are defined as follows:

$$F = \begin{pmatrix} 0 \\ 0 \\ f \end{pmatrix} \quad F_g = \begin{pmatrix} 0 \\ 0 \\ -mg \end{pmatrix} \tag{16}$$

The rotation matrix R is obtained from Euler angles in the order yaw-pitch-roll and it has the following expression:

$$R = \begin{pmatrix} c\psi c\theta & -s\psi c\phi + c\psi s\theta s\phi & s\psi s\phi + c\psi s\theta c\phi \\ s\psi c\theta & c\psi c\phi + s\psi s\theta s\phi & -c\psi s\phi + s\psi s\theta c\phi \\ -s\theta & c\theta s\phi & c\theta c\phi \end{pmatrix} \tag{17}$$

where $s = \sin(\cdot)$ and $c = \cos(\cdot)$. The yaw, pitch and roll angles are given by ψ, θ, ϕ, respectively. The Euler angles vector and the force vector u is defined as:

$$\eta = \begin{pmatrix} \psi \\ \theta \\ \phi \end{pmatrix} \quad u = \begin{pmatrix} u_x \\ u_y \\ u_z \end{pmatrix} \tag{18}$$

Then, from (2), (16), (17) and (18) it can be deduced the thrust and the Euler angles needed to generate the virtual control u^v. The ψ_{ref} needed can be chosen arbitrarily or conveniently. θ_{ref}, ϕ_{ref} and f_{ref} have the following expressions:

$$\theta_{ref} = \arctan\left(\frac{u_y s\psi + u_x c\psi}{u_z + mg}\right) \tag{19}$$

$$\phi_{ref} = \arctan\left(c\theta_{ref} \cdot \frac{u_x s\psi - u_y c\psi}{u_z + mg}\right) \tag{20}$$

$$f_{ref} = \frac{u_z + mg}{c\theta_{ref} \cdot c\phi_{ref}} \tag{21}$$

Let us define the Euler angles error as:

$$e_\eta = \eta - \eta_{ref} \quad \Longrightarrow \quad \begin{aligned} \dot{e}_\eta &= \dot{\eta} - \dot{\eta}_{ref} \\ &= B(\eta)\Omega - \dot{\eta}_{ref} \end{aligned} \tag{22}$$

The matrix $B(\eta)$ has the following form:

$$B = \begin{pmatrix} 0 & c\phi & -s\phi \\ 0 & s\phi/c\theta & c\phi/c\theta \\ 1 & s\phi \cdot t\theta & c\phi \cdot t\theta \end{pmatrix} \tag{23}$$

where t means $tan(*)$. The matrix $B(\eta)$ is not singular if and only if $\cos(\theta) \neq 0$.

Let us propose the next Lyapunov function

$$V_{L\eta} = \frac{1}{2} < \chi_2, K_{I\eta}\chi_2 > + \frac{1}{2} < e_\eta, e_\eta > \tag{24}$$

where,

$$\chi_2 = \int_0^t e_\Psi \, d\tau \tag{25}$$

and $K_{I\eta}$ is a positive diagonal constant matrix that will be used for tuning the control. Thus,

$$\dot{V}_{L\eta} = < \chi_2, K_{I\eta} e_\eta > + < e_\eta, \dot{e}_\eta > \tag{26}$$

and by choosing the virtual angular velocity Ω^v,

$$\Omega^v = B^{-1}\left(\dot{\eta}_{ref} - K_{I\eta}\chi_2 - K_\eta e_\eta\right) \tag{27}$$

with K_η as a positive diagonal constant matrix for tuning the control, it yields

$$V_{L\eta} = -K_\eta < e_\eta, e_\eta > \quad \leq 0 \quad \forall\ t \geq 0 \tag{28}$$

Now, let us define the angular velocity error as:

$$e_\Omega = \Omega - \Omega_\eta \quad \Longrightarrow \quad \dot{e}_\Omega = \dot{\Omega} - \dot{\Omega}_\eta \tag{29}$$

remember that,

$$\Omega = \Omega_\eta + e_\Omega \quad \& \quad \dot{\Omega} = \mathbb{J}^{-1}\left(\tau - \omega^\times \mathbb{J}\Omega\right) \tag{30}$$

Now, consider the following candidate lyapunov function:

$$V_{L\Omega} = V_{L\eta} + \frac{1}{2} < e_\Omega, e_\Omega > \tag{31}$$

so, then

$$\dot{V}_{L\Omega} = \dot{V}_{L\eta} + < e_\Omega, \dot{e}_\Omega > \tag{32}$$

thus,

$$\dot{V}_{L\Omega} = - < e_\eta, K_\eta e_\eta > + < e_\eta, B e_\Omega > + < e_\Omega, \dot{e}_\Omega > \tag{33}$$

and by choosing,

$$\tau = \omega^\times \mathbb{J}\Omega + \mathbb{J}\left(\dot{\Omega}_\eta - B^T e_\eta - K_\Omega e_\Omega\right) \tag{34}$$

it yields,

$$\dot{V}_{L\Omega} = - < e_\eta, K_\eta e_\eta > - < e_\Omega, K_\Omega e_\Omega > \quad \leq 0 \quad \forall\, t \geq 0 \tag{35}$$

with K_Ω as a positive diagonal constant matrix for the tuning of the control law, this strategy was taken from [13].

IV. Hardware and Experimental test

A. Hardware setup

Our prototype mini-UAV is based on the mechanical structure developed by FLEXBOT[1]. The attitude control law is executed on Flight Control System Microwii Copter Processor ATMega32u4, Gyro and Accel. Then, a ground station estimates the position and attitude of the mini-UAV using the Vicon system. With this system it is possible to compute the position and attitude up to 100Hz. The estimated states are sent to MATLAB/Simulink through a UDP frame every 2ms. The position control algorithm is implemented in real-time at 200Hz on a computer using xPC target toolbox . The control variables are finally sent back to the mini-UAV on the Microwii, through a GIPSA-lab's built-in bridge that converts UDP frames to Bluetooth protocol. The helmet is a TELEPORTER by fatshark [2]. The Vicon System [3] is used to obtain the 3D position and rotation (q) of the mini-UAV and the helmet. A PC (simulink) is used to compute the algorithm of velocity control. The data sample of simulink is arranged to 0.01 seconds. These components can be seen in the schema of the Fig.4 using the Vicon system. A video showing the experimental results can be viewed at [14].

[1]http://www.flexbot.com
[2]http://www.fatshark.com/
[3]Salle Moca, GIPSA-LAB

B. Experimental scenario

Two experiments were performed to evaluate the benefices of the control law defined in the section III. The objective is that the operator can operate the mini-UAV with the movements of the head. The orientation $(\phi_{head}, \theta_{head}, \psi_{head})$ of the helmet is used as reference of velocity input. In this experiments the operator only can move two meters in axes x and y because of the limited workspace. The attitude (axis z) of the mini-UAV is set to one meter. The specification and parameters of the mini-UAV prototype are given in the Table I.

TABLE I: The specification and parameters of the Quadrotor

Parameter	Description	Value	Units
m	Mass	0.057	Kg
d	Distance	0.042	m
J_x	Inertia in x-axis	0.0006833	Kg· m^2
J_y	Inertia in y-axis	0.0006833	Kg· m^2
J_z	Inertia in z-axis	0.00042993	Kg· m^2

1) Algorithm 1: The parameters of the control law are selected according to the characteristics of the actuators and those of the hexacopter presented previously. For the control (7) where max $\Gamma = 0.085Nm$ and $\Gamma_i = 0.04$, we obtain $\sigma_{123} = 0.04$, $k_{12} = 0.094$, $k_3 = 0.15$,$\rho_{12} = 0.022$ and $\rho_3 = 0.035$. For the control (15), $a_1 = a_2 = 1$ and $\bar{r}_1 2 = 1$, $\bar{r}_3 = 5$. The Fig. (5(a)) shows the behavior of the algorithm shown in section III-C.1 of position (Fig. 5(a)), attitude (Fig. 5(b)) and velocity (Fig. 5(c) and 5(d)).

The behavior of the first test (position, saturation control) can be seen in Fig. 5(a). We can see the trajectory of the mini-UAV which is commanded of the reference of velocity (ϕ_{ref} and θ_{ref}) is depicted in Fig. 5(c) and 5(d). The velocities (v_x, v_y) have a small delay (around 0.5 seg) with regard to reference (ϕ_{ref} and θ_{ref}). For this control the yaw angle is set to $\psi = 0$, only ϕ and θ can be changed to move the mini-UAV, see Fig. 5(b). We can see also that the performance is soft to the operator.

2) Algorithm 2: The second test (Control Law for Trajectory Tracking) is shown Fig. 6. The parameters of the control are $K_\eta = diag(4, 4, 4)$ and $K_\Omega = diag(1, 1, 1)$. In this case the operator can control the angle yaw (ψ, with head rotation see Fig. 6(b)). There is a delay of 0.25 seg to achieve the reference of the velocity.

V. Conclusion

This work proposes a teleoperation scheme to control a mini UAV using only head movements of operator. The position, orientation of the mini-UAV and the helmet movements are obtained using the Vicon System. The feasibility of this application was tested with two

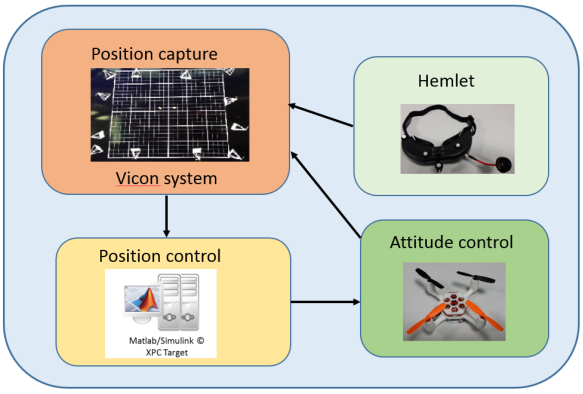

Fig. 4: Control System

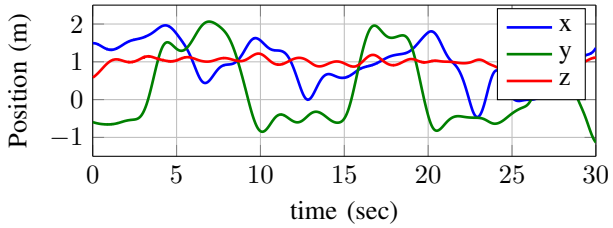

(a) Quadrotor Position

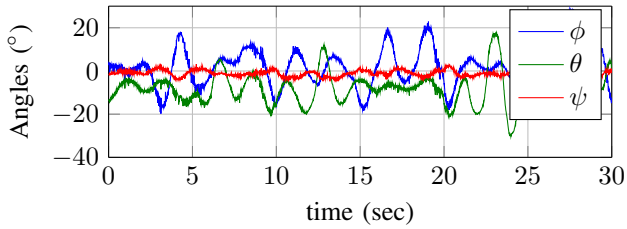

(b) Quadrotor Attitude

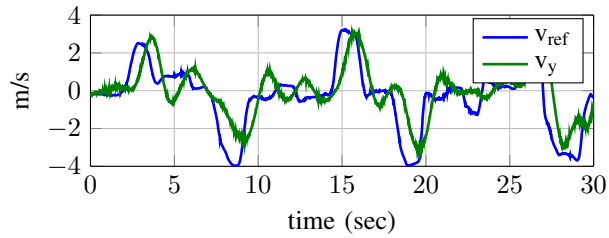

(c) ϕ_{head} and v_y

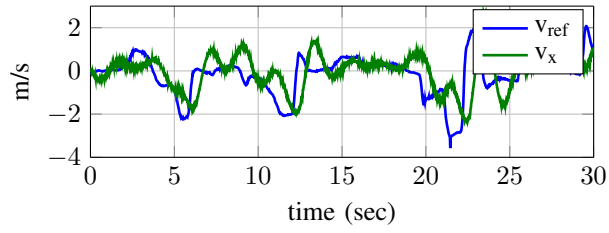

(d) θ_{head} and v_x

Fig. 5: Boundary Velocity Control with head movement

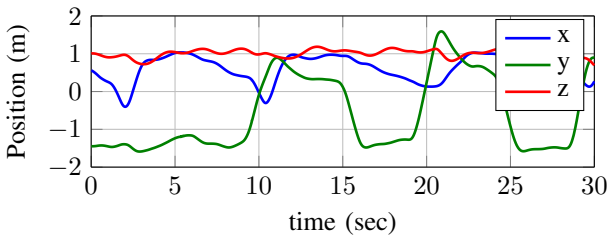

(a) Quadrotor Position

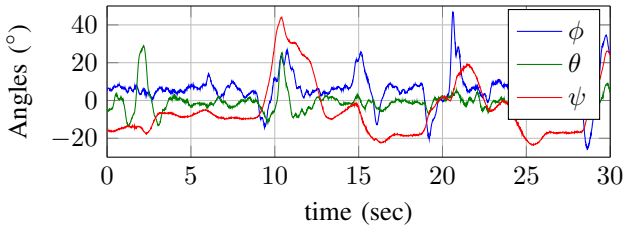

(b) Quadrotor Attitude

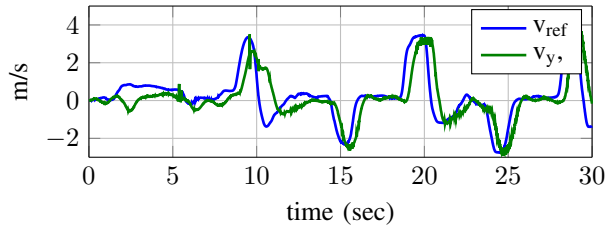

(c) θ_{head} and v_x

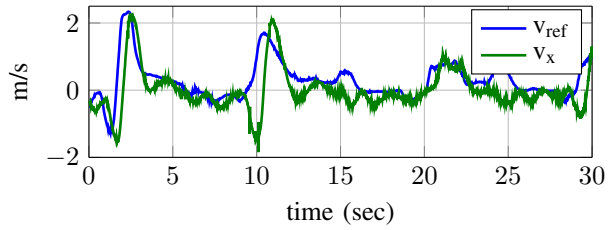

(d) ϕ_{head} and v_y

Fig. 6: Backstepping Velocity Control with head movement

algorithms of velocity. The manipulation of the mini-UAV with this method is more intuitive than using a radiocontrol. However, it has been noted that exists a delay of the signals sent from the operator to the mini-UAV. Even though this delay is imperceptible by the operator.

Both algorithms have similar results. Nevertheless, the position saturation control is soft and slow to the operation. Moreover the Control Law for Trajectory Tracking is more reactive and accurate for the follow-up of the movements of the operator. The second algorithm can also command the yaw angle (ψ) when the operator rotates the head.

In future works we will deep in the model operator and the implementation of feedback haptic forces. In order to

have a capable flying outdoors system without the Vicon system a vanishing point algorithm will be developed for the navigation in indoor environments.

ACKNOWLEDGMENT

The authors would like to thank the support and advice during the test of Bruno Boisseau and Ghatfan Hassan .

REFERENCES

[1] D. Lee, A. Franchi, H. I. Son, C. Ha, H. H. Bulthoff, and P. R. Giordano, "Semiautonomous haptic teleoperation control architecture of multiple unmanned aerial vehicles," *IEEE/ASME Trans. Mechatronics*, vol. 18, no. 4, pp. 1334–1345, 2013.

[2] H. I. Son, A. Franchi, L. L. Chuang, J. Kim, H. H. Bülthoff, and P. Robuffo Giordano, "Human-centered design and evaluation of haptic cueing for teleoperation of multiple mobile robots," *IEEE Trans. Cybern.*, vol. 43, no. 2, pp. 597–609, 2013.

[3] C. Masone, P. R. Giordano, H. H. Bülthoff, and A. Franchi, "Semi-autonomous Trajectory Generation for Mobile Robots with Integral Haptic Shared Control," pp. 1–8, 2014.

[4] T. M. Lam, V. D'Amelio, M. Mulder, and M. M. Van Paassen, "UAV tele-operation using haptics with a degraded visual interface," *Conf. Proc. - IEEE Int. Conf. Syst. Man Cybern.*, vol. 3, pp. 2440–2445, 2007.

[5] V. Grabe, M. Riedel, H. Bulthoff, and P. R. Giordano, "The TeleKyb Framework for a Modular and Extendible ROS-based Quadrotor Control," *2013 European Conference on Mobile Robots (ECMR) Barcelona, Spain*, 2013.

[6] P. Stegagno, M. Basile, H. H. Bülthoff, and A. Franchi, "A Semi-autonomous UAV Platform for Indoor Remote Operation with Visual and Haptic Feedback," pp. 3862–3869, 2014.

[7] R. Lozano, *Unmanned aerial vehicles: Embedded control*, 2013.

[8] K. . R. J. Higuchi, K.Fujii, "Flying head: A head-synchronization mechanism for flying telepresence," *Artificial Reality and Telexistence (ICAT), 2013 23rd International Conference on*, pp. 28 – 34, 2013.

[9] J. Teixeira, R. Ferreira, M. Santos, and V. Teixeira, "Teleoperation using Google Glass and AR.Drone for Structural Inspection," *XVI Symposium on Virtual and Augmented Reality IEEE*, pp. 28–36, 2014.

[10] J. Guerrero-Castellanos, N. Marchand, A. Hably, S. Lesecq, and J. Delamare, "Bounded attitude control of rigid bodies: Real-time experimentation to a quadrotor mini-helicopter," *Control Engineering Practice*, vol. 19, no. 8, pp. 790–797, 2011.

[11] J. Alvarez-Munoz, N. Marchand, J. Guerrero-Castellanos, S. Durand, and A. Lopez-Luna, "Improving control of quadrotors carrying a manipulator arm," in *XVI Congreso Latinoamericano de Control Automatico*, Cancun, Mexico, 2014.

[12] R. Cruz-José, J. F. Guerrero-Castellanos, W. F. Guerrero-Sánchez, and J. J. Oliveros-Oliveros, "Estabilización global de mini naves aéreas tipo vtol," in *Congreso Nacional de Control Automático*, Campeche, México, 2012.

[13] J. Colmenares Vazquez, N. Marchand, P. Castillo, and J. Gomez Balderas, "Integral backstepping control for trajectory tracking of a hybrid vehicle," in *International Conference on Unmanned Aircraft Systems*, Denver, CO, USA, June 2015.

[14] J. Tellez-Guzman, "Test," 2015. [Online]. Available: $https$: $//www.dropbox.com/s/qb2040e9ox2vf62/VelocityC_G.mp4?dl = 0$